Microsc. Microanal. 24 (Suppl 1), 2018
doi:10.1017/S1431927618007067

Fluorescence Microscopy as a Tool for Nanomedicine-Cell Interactions Study: Input of Particle Design and of Analytical Strategy

Sanaa Ben Djemaa[1], Mathias Pacaud[1,2], Katel Hervé-Aubert[1], Stéphanie David[1], Emilie Allard-Vannier[1], Emilie Munnier[1], Anastasia Ignatova[3], Amir Fahmi[2], Alexey Feofanov[3,4] and Igor Chourpa[1]

[1.] EA6295 Nanomedicine & Nanoprobes, University of Tours, Tours, France.
[2.] Faculty Technology&Bionics, Rhein-Waal University of Applied Sciences, Kleve, Germany.
[3.] Shemyakin and Ovchinnikov Institute of Bioorganic Chemistry, Russian Academy of Sciences, Moscow, Russia.
[4.] Biological Faculty, Lomonosov Moscow State University, Moscow, Russia.

Various nanomedicine platforms are developed in perspective of disease diagnosis, therapy or theragnosis, namely those based on superparamagnetic iron oxide nanoparticles (SPIONs) and/or gold nanoparticles (AuNPs) [1]. For each nanomedicine platform, one of critical parameters to evaluate is its interaction with target cells, namely its adhesion to cell surface, its internalization, subcellular distribution and action mechanism(s) [2-4]. For this kind of studies, optical microscopy is often used, as it provides physiological and complete view of cells. Some of AuNPs and AgNPs can be detected by dark field microscopy, due to plasmon-enhanced scattering of light. For more specific and spatially resolved optical microscopy of a wide range of metal NPs (MNPs), usual strategy consists in labelling them with fluorescent dyes and detecting them with laser scanning confocal microscopy (LSCM). However, in order to take benefit of the fluorescence microscopy and make relevant conclusions from it, choice of an appropriate particle design and analytical strategy are critical.

Based on our recent studies of fluorescent MNPs coated with various organic shells, we have established several rules [2-4]. First of all, they concern the MNPs fluorescent labelling: (i) covalent binding of the dye can be not enough to ensure its chemical stability – it can be degraded and/or detached from the MNP inside cells; (ii) the dye covalently bound to the MNP core should be hidden under the organic shell (typically under the polymer like polyethylene glycol, PEG), otherwise it can be cleaved from the particle and/or quenched, as well as it may affect the colloidal stability of the particle and its interactions with biological targets. Secondly, relevant assessment of nanoparticle behavior within cells is also dependent on the ability to distinguish the fluorophore attached to the nanoparticles from that one detached from them. The latter is also very important to follow delivery of fluorescent active molecules.

We describe here two analytical strategies helpful in understanding of the fluorescence originating from cells treated with nanomedicine platforms. The first one consisted in using confocal spectral imaging (CSI, made with a LabRam microscope, Horiba SA, France) of the fluorescence (Fig 1): recording full spectra of AlexaFluor488-labelled siRNA from each point of the cell scanned with excitation laser beam (491 nm line of a Calypso 75 laser, Cobolt, France) allowed us to map separately the siRNA loaded into SPION-PEG and the siRNA released to the cytosol (em max at 521 and 527 nm, respectively, Fig 1 C).

The second strategy consisted in adjusting non-spectral LSCM microscope (Model SP2, Leica, Germany) for complementary spatially-resolved analysis of the elastic scattering from AuNPs (633 nm) together with the fluorescence from the Nile Blue dye (exc/em 633/(670-676) nm). This allowed us to establish that MNPs remain attached on the cellular membranes while the released dye enters the cells and accumulated in cytoplasmic vesicles (Fig 2).

To conclude, rational particle design together with innovative analytical approaches based on laser-scanning confocal microscopy (spectral and non-spectral detection of fluorescence and of light scattering) contribute into a reliable understanding of nanomedicine-cell interactions [5].

References:

[1] J Gautier et al. J Control Release **169**(1-2) 2013, p. 48.
[2] J Bruniaux et al. Int J Pharm. **S0378-5173**(17) (2017), p. 30432.
[3] E Allard-Vannier et al. Biochim Biophys Acta **1861**(6) (2017), p. 1578.
[4] E Perillo et al. J Colloid Interface Sci. **499** (2017), p. 209.
[5] The authors acknowledge funding from the following grants in the frames of MINERVA project (ERA-NET RUS PLUS program): RFBR 16-54-76013 (Russia), 01DJ16019 (Germany) and MENESR N°321 (France). We acknowledge also the support from Institut National du Cancer (INCa), Fondation ARC and Ligue Nationale Contre le Cancer (LNCC) (grant ARC_INCa_LNCC_7636).

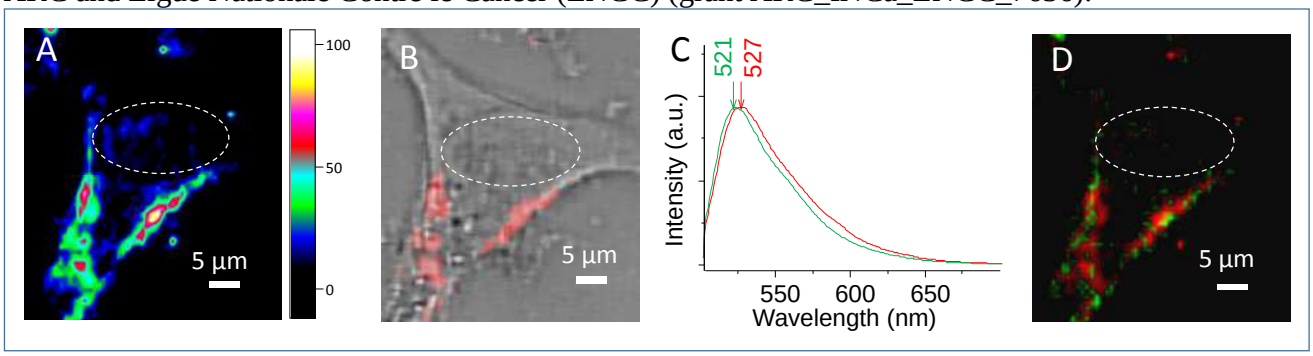

Figure 1. Delivery of siRNA to a live BT474 cancer cell by SPION-PEG nanovectors as studied by CSI: A - map of the total fluorescence intensity distribution over the cell (dashed line indicates nucleus); B – merge of the map A (red zones) with a white-light image of the cell; C – typical fluorescence emission spectra from Alexa 488-labelled siRNA loaded to the nanovectors suspended in PBS (green line) and once delivered to cytosol (red line); D: merge of two spectral maps: siRNA still carried by the nanovectors (green zones seen on the cell membrane) and siRNA released to cytosol (red zones).

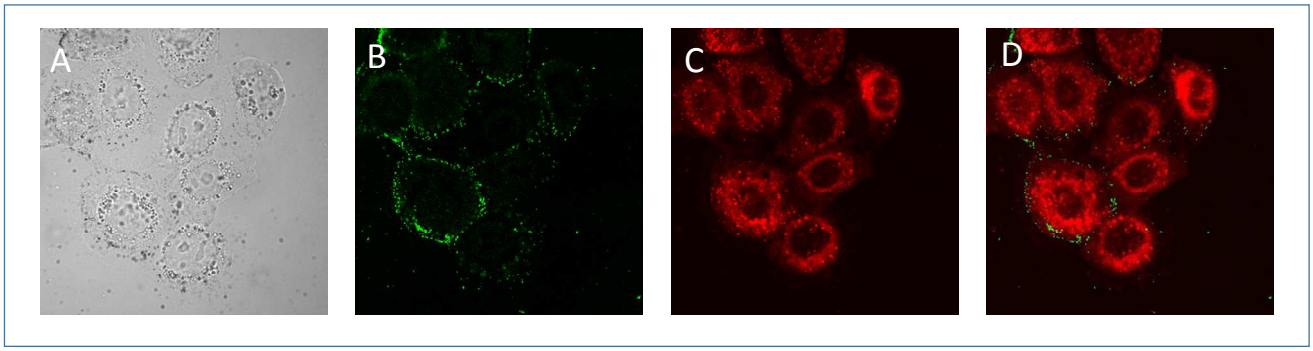

Figure 2. Delivery of fluorescent dye Nile Blue (NB) to SKBR3 cancer cells by plasmonic gold nanoparticles (AuNPs) as studied by LSCM: A – white-light image of cells; B – plasmon-enhanced elastic scattering image shows that AuNPs are mainly accumulated on cell membrane; C – far red fluorescence of NB shows that the dye is internalized and accumulated in vesicular cytoplasmic structures. D – merge of the B and C images.